COMPDYN 2017
6th ECCOMAS Thematic Conference on
Computational Methods in Structural Dynamics and Earthquake Engineering
M. Papadrakakis, M. Fragiadakis (eds.)
Rhodes Island, Greece, 15–17 June 2017

RINTC PROJECT: NONLINEAR DYNAMIC ANALYSES OF ITALIAN CODE-CONFORMING URM BUILDINGS FOR COLLAPSE RISK ASSESSMENT

D. Camilletti[1], S. Cattari[1], S. Lagomarsino[1], D. Bonaldo[2], G. Guidi[2], S. Bracchi[3], A. Galasco[3], G. Magenes[3], C.F. Manzini[3], A. Penna[3] and M. Rota[3]

[1] Dept. of Civil, Chemical and Environmental Engineering, University of Genoa, Via Montallegro 1, Genoa, Italy
e-mail: danicami.dc@gmail.com, {serena.cattari,sergio.lagomarsino}@unige.it

[2] Dept. of Civil, Environmental and Architectural Engineering, University of Padova, Via Marzolo 9, Padua, Italy
{diego.bonaldo,giovanni.guidi}@dicea.unipd.it

[3] European Centre for Training and Research in Earthquake Engineering, Via Ferrata 1, Pavia, Italy and Dept. of Civil Engineering and Architecture, University of Pavia, Via Ferrata 3, Pavia, Italy

e-mail: {stefano.bracchi,alessandro.galasco,carlo.manzini,guido.magenes,andrea.penna, maria.rota}@eucentre.it

Keywords: Unreinforced masonry, Nonlinear static and dynamic analysis, Equivalent frame models, Multi-stripe analysis, Collapse estimate.

Abstract. *This paper deals with the computation of the collapse risk of new masonry buildings designed according to the Italian Building Code. Companion papers describe the overall EUCENTRE-ReLUIS joint research project, funded by the Italian Department of Civil Protection (DPC), which considers different building types (r.c., steel buildings, etc) and uses multi-stripe nonlinear dynamic analyses by properly selected ground motion records. 2- and 3-storey unreinforced masonry buildings have been designed in cities with increasing seismic hazard, considering two different soil conditions at each site. First, the paper describes geometry, material characteristics (clay block masonry) and main structural details of the buildings, discussing the effect of different design methods (rules for simple buildings, linear and nonlinear static analysis) and models (cantilever or equivalent-frame models). The models used for the assessment by nonlinear dynamic analyses are equivalent-frame models made by masonry piers and spandrels, as well as reinforced concrete members. Two alternative macroelement models are used for the in-plane response of masonry members. Out-of-plane failure modes are assumed to be prevented by the presence of ring beams and limited slenderness of masonry walls. Pushover analyses are used to esti-mate the EDP (maximum interstorey drift ratio) threshold for the collapse limit state. Finally, the results of the multi-stripe analyses are presented for 10 different earthquake's return periods.*

1 INTRODUCTION

RINTC is a joint project of ReLUIS and EUCENTRE, two centers of competence for seismic risk assessment of the Italian civil protection [1]. The goal of the project is to assess in an explicit manner the seismic risk of structures designed according to the code currently enforced in Italy. Five structural typologies were considered: masonry, reinforced concrete, pre-cast reinforced concrete, steel, and seismically isolated buildings. The final aim is to check whether code provisions are able to produce buildings with a uniform seismic risk, both considering sites characterized by a different earthquake hazard and adopting different structural materials and technologies. Different case study buildings have been tightly safe designed by means of the current engineering-practice methods.

The distinctive feature of masonry buildings, which this paper focus on, is that many alternative design procedures are considered in the Italian building code [2] and widely used by engineers. This leads to the design of different structural configurations (thickness of wall, quality of masonry units and mortar) for the same architectural layout, depending on the adopted method (rules for simple buildings, linear or nonlinear static analysis with cantilever or equivalent-frame models). In the selection of case studies for masonry, both regular and irregular configurations (in plan and/or in elevation) have been considered.

The risk assessment in terms of global failure was performed by nonlinear dynamic analyses with two alternative constitutive models [3,4] implemented within the framework of an equivalent frame model [5]. Both able to consider the stiffness and strength degradation of the masonry panels and the cyclic hysteretic behavior, specific for the different failure modes (rocking, diagonal cracking, sliding and hybrid) of piers and spandrels.

The Engineering Demand Parameter (EDP) selected to identify the masonry building performance is the maximum wall inter-story drift. Limit thresholds have been evaluated from pushover analysis, by considering specific values for each building configuration and distinguishing the behavior in the two orthogonal directions.

Some typical results are shown, in terms of global cyclic behavior under dynamic actions, progressive increase of the limit state function with the intensity measure and percentage of collapse in the different sites. The results of failure risk calculation are presented in [1].

2 DESIGN OF ITALIAN-CODE CONFORMING URM BUILDINGS

2.1 Case study structures

The analyzed structures are associated with eight different (in plan) architectural configurations, which were designed according to the rules of the Italian building code [2].
All the designed configurations are two- or three-story unreinforced masonry buildings, made of vertically perforated clay units with mortar head- and bed-joints.

Based on the definition of “regularity in plan” and “regularity in elevation” provided by NTC 2008, the architectural configurations examined have been divided into two main categories: regular and irregular. Figure 1 and Figure 2 show, respectively, the regular and the irregular plan configurations considered. A brief description of each architectural configuration is provided in the following:

- “C” type configuration (regular, two and three-story): flat roof, inter-story height of 3.10 m.

- "E" type configurations (regular and irregular, two and three stories): four configurations, three of which are regular in plan and elevation (E2, E8, E9), whereas one has a limited degree of irregularity in plan (E5). The inter-story height is 3.10 m and the roof is pitched, sloping at 19° with eaves protruding 1.30 m from of the external side of the outer walls.
- "I" type configurations (irregular, two and three-story): the two-story building (I1) presents only plan irregularity, with inter-story height of 3.30 m, the three-story building (I2) is also irregular in elevation, with inter-story of 3.10 m. In both cases, the roof is flat.
- ''F'' type configurations (irregular in plan and elevation, two-story): RC slabs at intermediate levels and a roof made of a wooden truss and a lightweight concrete slab. The inter-storey height is 3.0 m at ground floor and 3.2 m at first floor.
- "G" type configurations (irregular in plan and elevation, three-story): "L" shape in plan. The roof at both lower levels is made of 4 cm thick concrete slabs, supported on masonry parapets, at the third level is a composite wood-lightweight concrete roof. The inter-story height is 3.0 m at all levels.

All considered configurations (types "C", "E", "F", "G", "I") have some common or similar features, i.e. mechanical properties of materials, minimum thickness of bearing walls, geometry of ring beams. Slabs made of combined concrete and hollow clay blocks (20+4 cm solution) have been used for all diaphragms. Moreover, all the configurations have r.c. ring beams at each level, with the minimum reinforcement allowed by the code, i.e. four 16 mm rebars of longitudinal reinforcement and 8 mm stirrups every 25 cm. According to NTC 2008, the ring beams of internal walls are as large as the wall, whereas those of the external walls are 5 cm shorter than the thickness of the wall, to accommodate thermal insulation elements.

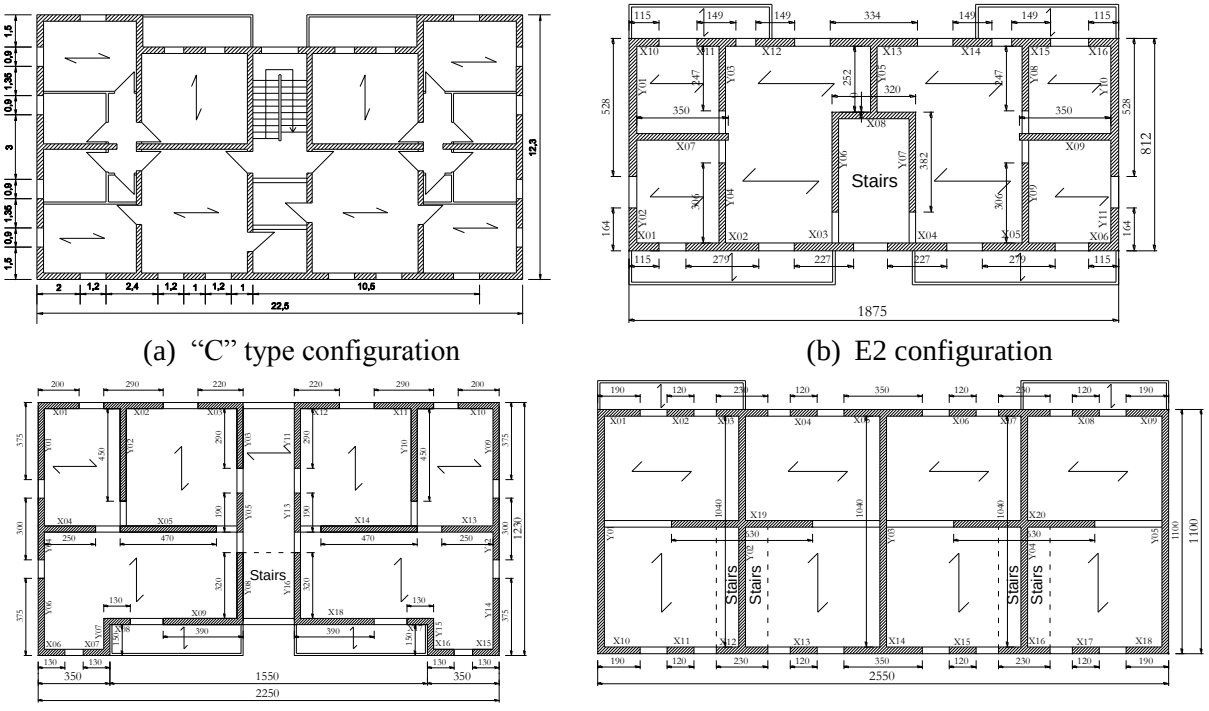

(a) "C" type configuration (b) E2 configuration

(c) E8 configuration (d) E9 configuration

Figure 1: Selected case studies – regular architectural configurations

The mechanical properties of the materials used for the defined configurations are summarized in Table 1.

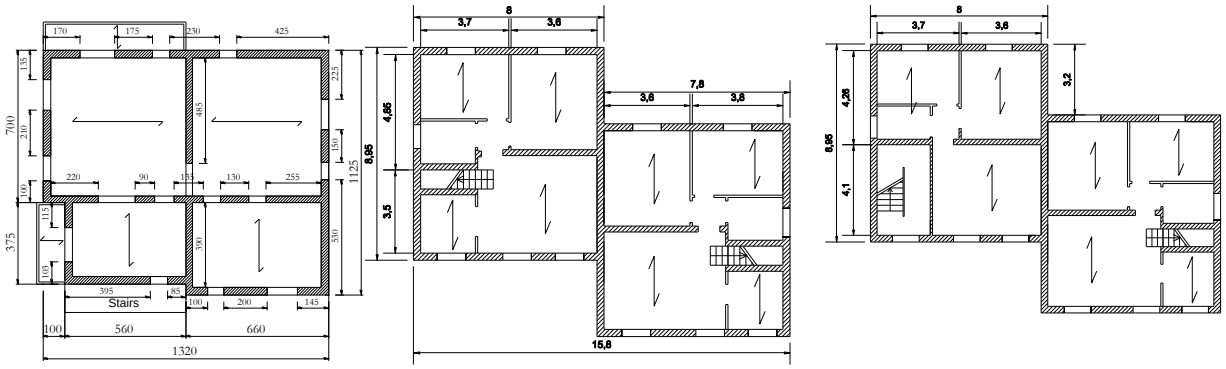

(a) E5 configuration (b) I1 configuration (c) I2 configuration

(d1) "F" type configuration - Ground floor (d2) "F" type configurations - 1st floor

(e1) "G" type conf. - ground floor (e1) "G" type conf. – 1st floor (e1) "G" type conf. – 2nd floor

Figure 2: Case studies selected – irregular architectural configurations

2.2 Design criteria and results

Masonry buildings are typically designed using different analysis methods depending on the level of seismicity of the site. This is due to the high level of conservatism implicit in linear analysis methods, which are practically unusable in sites with moderate to high seismicity. On the other hand, nonlinear static analysis is commonly used in practice even for design, thanks to the availability of dedicated software. The other design procedure commonly adopted in practice is based on the application of "simple building" rules.

For each one of the sites considered in this project (5 sites and 2 soil types, for a total of 10 sites, see [1]), the different plan configurations presented in the previous section were designed/selected with the aim of identifying the optimal solutions, which were able to barely comply with the code requirements at the site. This procedure was repeated for the different analysis methods and modelling approach considered, to be able to compare the results obtained in the different cases.

Configuration type		**C/I**	**E**	**F**	**G**
Young modulus	E	$1000 \cdot f_k$	$1000 \cdot f_k$	$1000 \cdot f_k$	$1000 \cdot f_k$
Shear modulus	G	$0.4 \cdot E$	$0.4 \cdot E$	$0.4 \cdot E$	$0.4 \cdot E$
Compressive strength of units	f_{bk} *[MPa]*	8	8	8 ÷ 15	15
Horizontal compressive strength of units	f'_{bk} *[MPa]*	1.5	1.5	1.5	1.5
Specific weight	w *[N/m^3]*	9000	9000	11000	11000
Mortar class	-	M10	M10	M5-M10	M10
Characteristic compressive strength of masonry	f_k *[MPa]*	4.66	4.66	4.22÷6.7	6.7
Design compressive strength (for gravity loads)	f_d *[MPa]*	$f_k/3$	$f_k/3$	$f_k/3$	$f_k/3$
Design compressive strength (for seismic loads)	f_d *[MPa]*	$f_k/3$	$f_k/2$	$f_k/2$	$f_k/2$
Shear strength w/o vertical load	f_{vk0} *[MPa]*	0.2	0.2	0.2	0.2
Compressive strength of concrete	f_{ck} *[MPa]*	20	25	25	25

Table 1: Mechanical properties of the materials used in the defined configurations.

The considered analysis approaches, in accordance with NTC08, consist of:

- Linear static analysis (LSA) with either equivalent frame (LSA_F) or cantilever (LSA_C) modelling
- Nonlinear static analysis (NLSA) based on equivalent frame modelling
- Rules for "simple" masonry buildings (SB)

However, these analysis methods were not applied to all building configurations. For example, "F" "G" and "I" configurations were not designed with simple building rules because they are irregular structures, in plan and/or in elevation.

Regarding "C" type configurations, 7 different plan arrangements (from C1 to C7, Figure 3) were considered, by varying the percentage of resistant area (gradually increasing from 4% to 7%, depending on the seismic input and the number of stories). The different percentages of resistant area were obtained by varying the thickness of the masonry walls (internal and external) from a minimum of 25 cm to a maximum of 40 cm. Furthermore, in C1 and C2, some internal walls were replaced by RC beams and columns, to reduce the percentage of resistant area. The different arrangements were conceived to guarantee a safety index slightly larger than 1, according to the various design methods adopted.

The "E" type and "I" type configurations considered are reported in Figure 1 and Figure 2. Regarding the "F'' and "G" type configurations, different building layouts were designed, by varying the width of the walls (from 25 to 40 cm), the mechanical characteristics of masonry, the length and position of door and window openings, substitution of internal partitions by load bearing walls. The configurations considered are shown in Figure 4 and Figure 5.

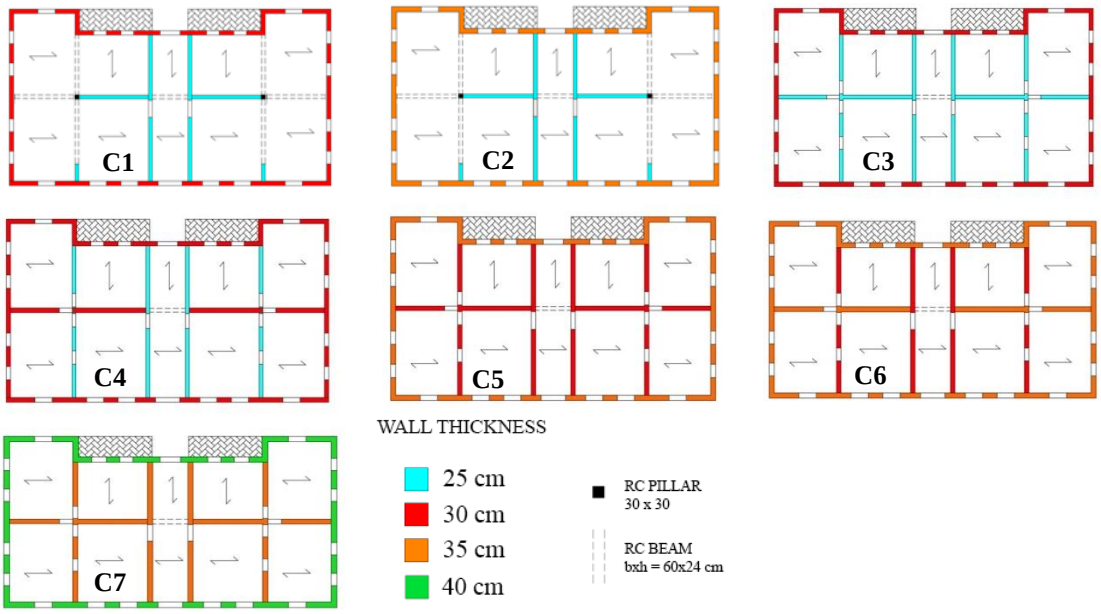

Figure 3: Plan configurations of the ground floor of the ‘’C’’ type buildings

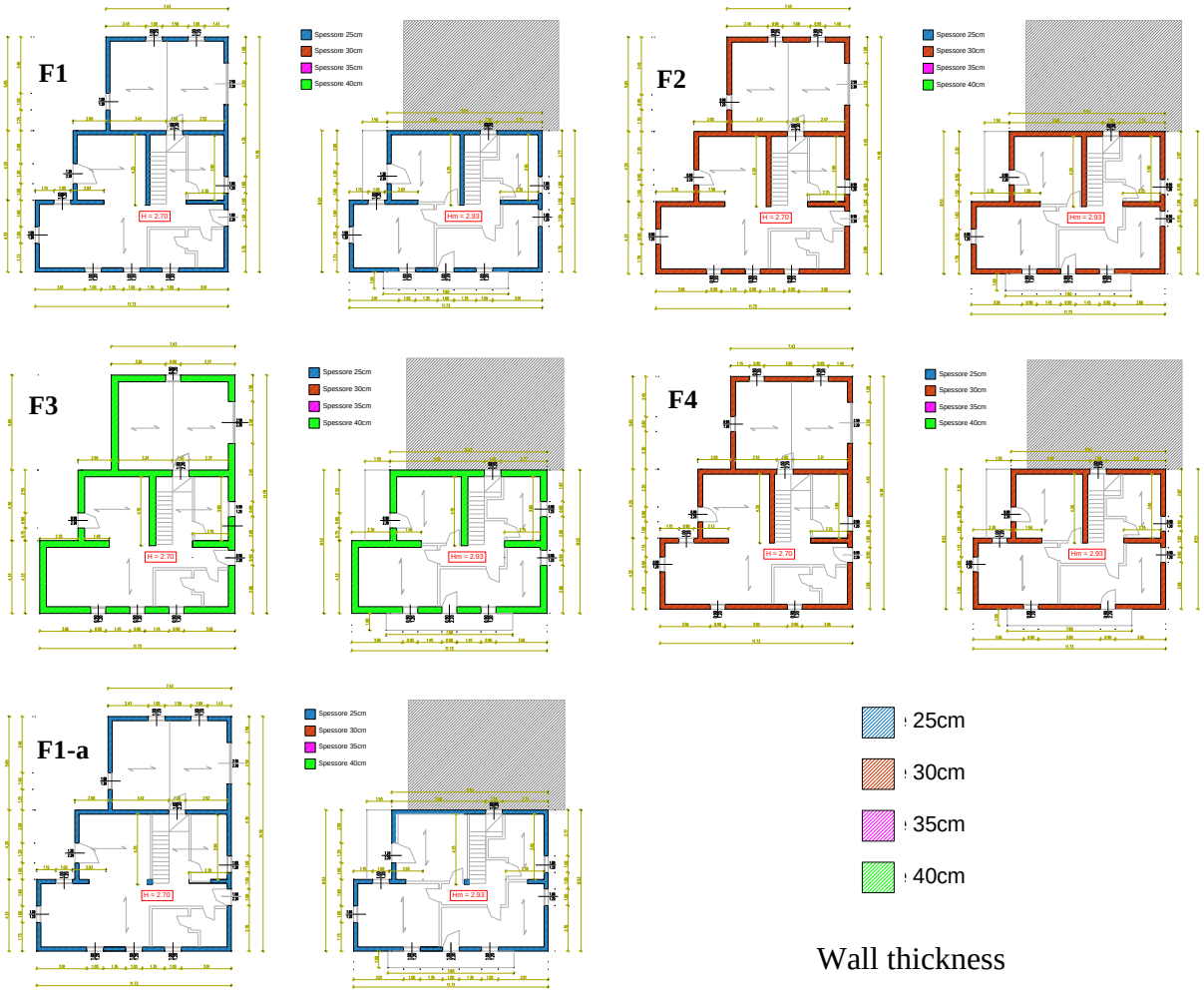

Figure 4: Plan views of the different ‘’F’’ type configurations considered

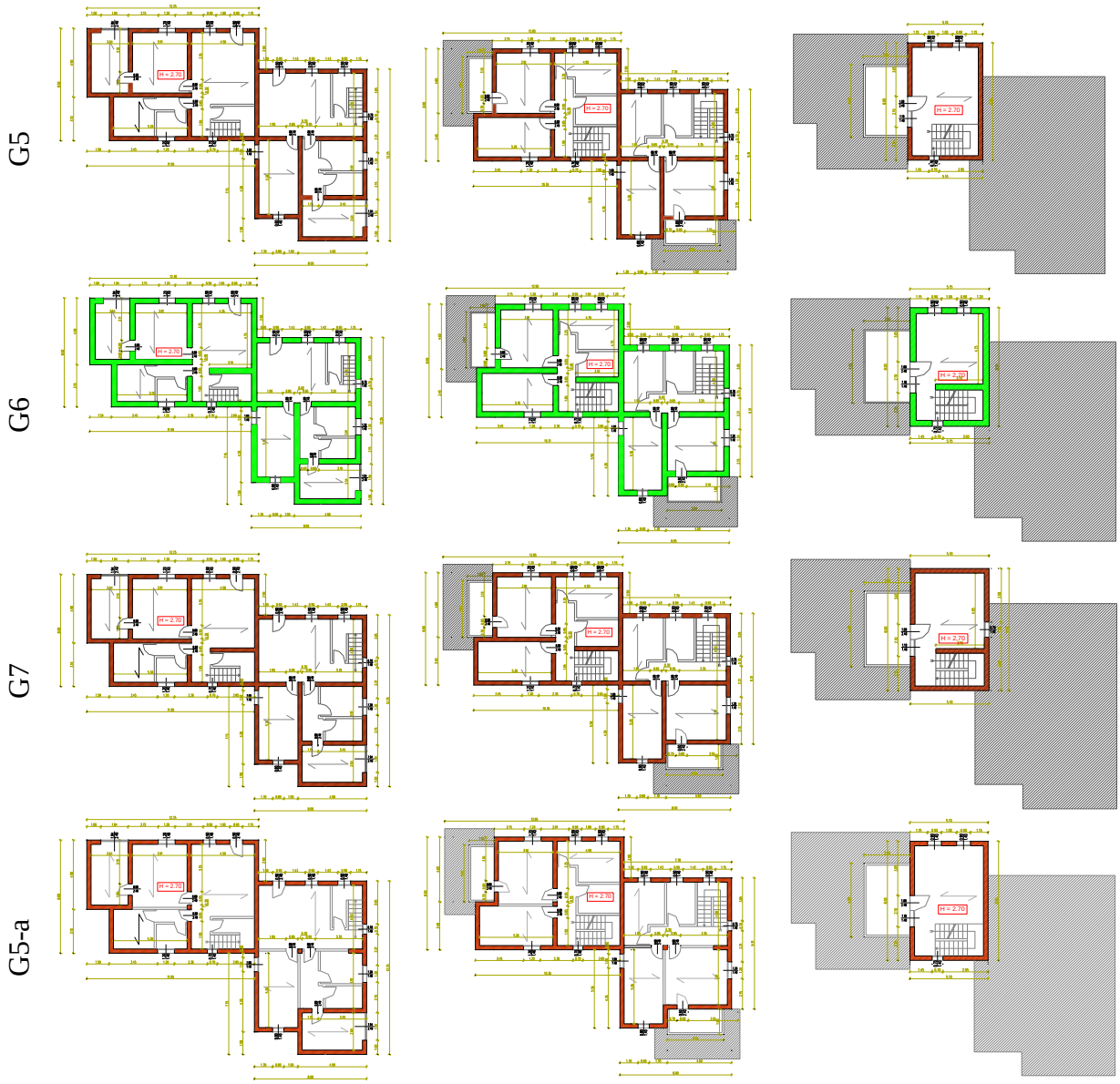

Figure 5: Plan views of the different ‘’G’’ type configurations considered

Table 2 summarises the design results, in terms of building configurations barely complying with code requirements, obtained for each considered site and for each analysis method.

The results obtained show that buildings designed with linear static analysis are often complying only for lower seismicity sites. In many cases, buildings do not even satisfy the requirements for the site of Milan and for soil type A, due to the occurrence of localized failures in a limited number of elements, since the very first analysis steps. However, it is worth mentioning that in these cases no force redistribution was applied. On the other hand, if the same buildings that barely comply using LSA are designed with nonlinear static analysis, they result to largely comply with the requirements, in particular in case of two-storey buildings and often even for higher seismicity sites.

		2-storey buildings				3-storey buildings			
Site	a_gS [g]	LSA_C	LSA_F	SB	NLSA	LSA_C	LSA_F	SB	NLSA
Mi_A	0.049	C4, E2, E5, F2, F4, G7	C4, E5, F1, F2, F4	C1	C1, I1	C6, E2, E5, G7	E5, G6, G7	C2	C1, I2, G5-a
Mi_C	0.074	F3	C7, E2, F2, G5, G6, G7	C2	C1, I1	E8, E9	E2, E9	C3, E9	C1, I2
Cl_A	0.073	F3	C7, E2, F2, F4, G5, G6, G7	C1	C1, I1	E8, E9	E2, E9, G7	C2, E9	C1, I2, G5
Cl_C	0.109	-	E8, E9, F3	C2, E9	C1, I1, F1-a	-	E8	C3, E8	C1, I2
Rm_A	0.121	-	E8, E9, F3	C2, E9	C1, I1	-	E8	C3, E8	C1, I2, G6
Rm_C	0.182	-	-	C3, E8	C1, I1	-	-	C4	C1, I2
Na_A	0.168	-	-	C3, E8	C1, I1	-	-	C4	C1, I2, E5
Na_C	0.245	-	-	C4	C1, I1, F1	-	-	C5, E2	C3, I2, E2, E8
Aq_A	0.261	-	-	E2	C1, I1, F2, F4	-	-	-	C1, E2, E8
Aq_C	0.347	-	-	-	C3, I1, E2, E5, E8, E9, F2, F3, F4	-	-	-	-

Table 2: Building configurations designed to barely comply with code requirements, for each of the considered sites (Mi = Milan, Cl = Caltanissetta, Rm = Rome, Na = Naples, Aq = L'Aquila; subscript "A" and "C" refer to the soil type) and for each analysis method (SB = simple building, LSA_F and LSA_C = linear static analysis with equivalent frame or cantilever models, NLSA = nonlinear static analysis).

3 MODELLING ISSUES FOR THE SEISMIC ASSESSMENT

The different designed building models were assessed by nonlinear dynamic analyses (NLDA), using the records selected by Iervolino et al. [1], for each site and for 10 values of return period of the seismic action. The aim was to evaluate the actual safety with respect to the collapse condition.

Analyses were carried out using the Tremuri computer program [5], with an equivalent frame approach. The constitutive laws defined for NLDA allow the simulation of:

- stiffness and strength degradation of the masonry panels composed by hollow clay blocks and cement mortar characterizing the considered buildings;
- a cyclic hysteretic behavior, specific for the different failure modes (rocking, diagonal cracking, sliding and hybrid) of piers and spandrels.

This required a review of the experimental data available in the literature for such masonry type, to calibrate the constitutive laws and to derive drift limits and strength degradation thresholds, for shear and flexural failure modes, in order to provide as much as possible a reliable simulation of the actual behavior expected. All the considered experimental results refer to piers' response, as tests on spandrels composed by modern blocks are too limited to permit

meaningful statistical evaluations. Nevertheless, the uncertainty in the definition of drift limits for spandrels does not significantly affect the analyses performed, since the contribution provided by reinforced concrete beams in coupling piers was dominant. In fact, differently from existing buildings, the interaction with r.c. elements promotes a "strong spandrels" behavior, with nonlinearity mainly concentrated in piers. Based on experimental results [6-8], drift limits for the shear behavior of 0.24% for the ultimate limit state (20% drop of maximum lateral strength) and of 0.54% for the near collapse condition (50% drop) were adopted. Drift limits for the flexural behavior of 1.22% for ultimate limit state (based on [9]) and 1.6% for collapse condition (assumed as 4/3 of the ultimate limit state) were adopted. In case of hybrid failure modes, experimental tests suggest the adoption of intermediate drift limits.

The two different approaches used to model masonry panels are discussed in the following sections. They consist of an approach based on a phenomenological nonlinear beam [3] and a mechanics-based macroelement model [4]. Both are implemented in the Tremuri program [5], selected for performing NLDA.

3.1 Nonlinear beam with piecewise-linear force-deformation relationship

In this model [3], masonry panels are modelled as nonlinear beam elements with lumped inelasticity and a piecewise-linear behavior. The constitutive law allows describing the nonlinear response until very severe damage levels (from 1 to 5), through progressive strength degradation at assigned values of drift (Figure 6a). The hysteretic response (Figure 6b) is formulated through a phenomenological approach, allowing to capture the differences among the possible failure modes (mainly flexural. shear or hybrid) and the different response of piers and spandrels.

Two sets of parameters are required (Table 3): the first one describes the backbone curve, whilst the second one defines the hysteretic response. The first set includes parameters defining the initial stiffness of the panel and its progressive degradation (defined starting from the secant stiffness, by two coefficients k_r and k_0), the maximum strength of the panel (V_u) and the progressing of the nonlinear response for increasing damage levels (δ_{Ei}, β_{Ei}).

The maximum strength of the panel (V_u) is computed as the minimum value obtained with simplified criteria for the different failure modes (flexural, shear, or hybrid) consistent with those recommended in standards [2] or proposed in the literature [10-11]. Different values of $\theta_{E.i}$ and $\beta_{E.i}$ may be defined in case of prevailing flexural or shear response of the panel, as well as in case of spandrels and pier elements.

The second set of parameters describes the hysteretic response, by defining the slope of the unloading and loading branches of the hysteresis loops.

With reference to Figure 6b, the unloading branch from A+ to C+ is governed by the stiffness K_u. For example, in case of positive quadrant, it is computed as:

$$K_u^+ = K_{sec}\left(\mu^+\right)^{\alpha}\left[1-\zeta\left(1-\beta_i^+\right)\right] \tag{1}$$

where μ^+ is the maximum value of ductility reached in the backbone of the positive quadrant; α is a parameter degrading the value of K_u with respect to the secant stiffness K_{sec} (it may assume values from 0 - elasto-plastic law- to 1 -secant stiffness); ζ aims at further degrading the value of K_u, taking into account the progressing strength decay reached on the backbone. An analogous expression may be defined for the negative quadrant.

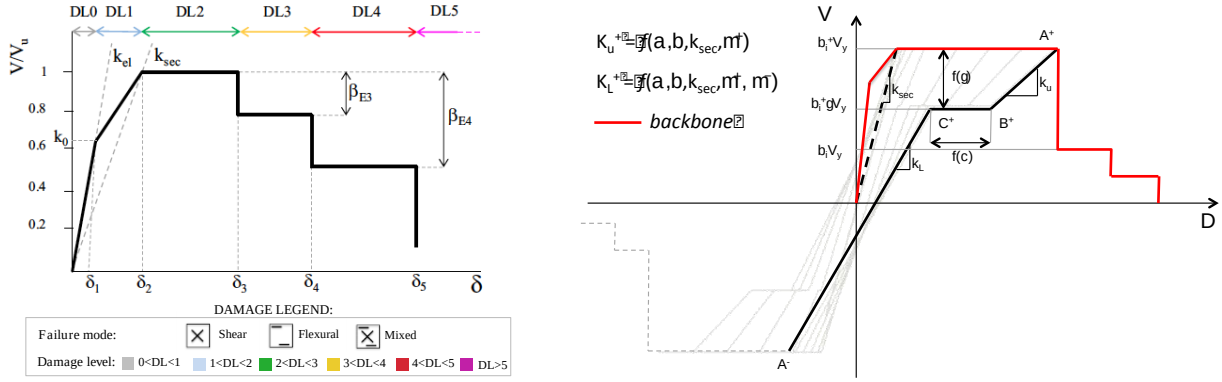

(a) (b)

Figure 6: Piecewise linear constitutive law: backbone curve (a) and hysteretic response (b)

After a first branch (A+ B+) governed by K_u, the unloading branch may also exhibit a horizontal branch (B+ C+), where the point B^+ is determined by the γ coefficient, which varies from 0 (A^+ B^+ branch until the x axis) to 1 (elastic nonlinear condition). The extension of B^+ C^+ is determined by the χ coefficient, which may vary from 0 to ∞, although suggested values range from 0 to 1.

Finally, the loading branch from C+ to A- is governed by the stiffness K_L, computed by considering K_u and the maximum ductility value reached in both positive and negative quadrants (μ+, μ-).

Table 3 summarizes the parameters adopted in NLDA.

	Shear						Flexure					
	Pier			Spandrel			Pier			Spandrel		
	DL3	DL4	DL5	DL3	DL4	DL5	DL3	DL4	DL5	DL3	DL4	DL5
Drift [%]	0.24	0.54	0.7	0	0.4	0.7	0.6	1.22	1.6	0.6	0.8	1.2
Residual strength [%]	0.6	0.2	0	0.7	0.7	0	1	0.85	0	1	0.7	0
α	0.8			0.2			0.9			0.2		
β	0.8			0			0.8			0		
γ	0			0.3			0.6			0.3		
χ							0.5			0.8		

Table 3: Parameters adopted for NLDA for piers and spandrels. with the piecewise linear constitutive law

Figure 7 shows the hysteretic response simulated by NLDA, for three wall panels with fixed-fixed boundary conditions, subjected to a compressive state equal to 7% of the masonry compressive strength, with three different slenderness ratios. to induce different failure modes (flexural, shear or hybrid).

3.2 Macroelement mechanical model

The second model which has been adopted is based on the effective nonlinear macroelement modelling approach [4]. The macroelement model represents the cyclic nonlinear behavior associated with the two main in-plane masonry failure modes, bending-rocking and shear mechanisms, with a limited number of degrees of freedom (8) and internal variables which describe the damage evolution. The two-node mechanics-based microelement, suitable for

modelling piers and spandrel beams, can be ideally subdivided into three parts: a central body where only shear deformation can occur and two interfaces where the external degrees of freedom are placed, the latter being able to exhibit relative axial displacements and rotations with respect to those of the extremities of the central body. In the two interfaces, infinitely rigid in shear, the axial deformations are due to a distributed system of zero-length springs with no-tension and limited compression behavior.

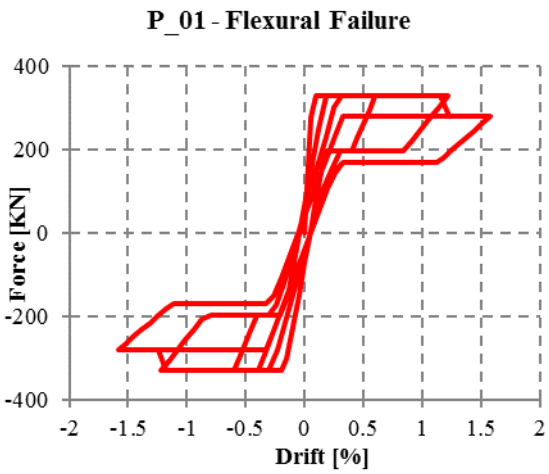

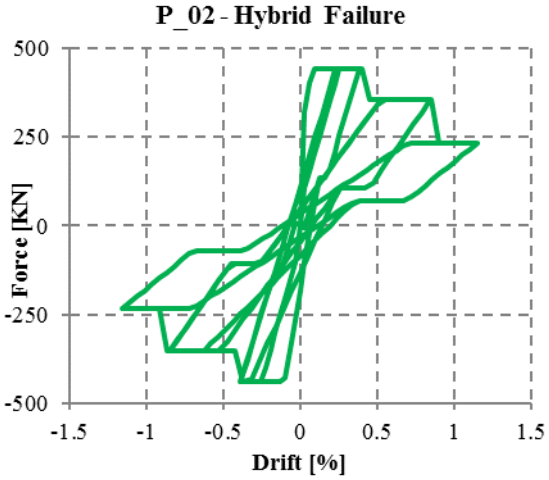

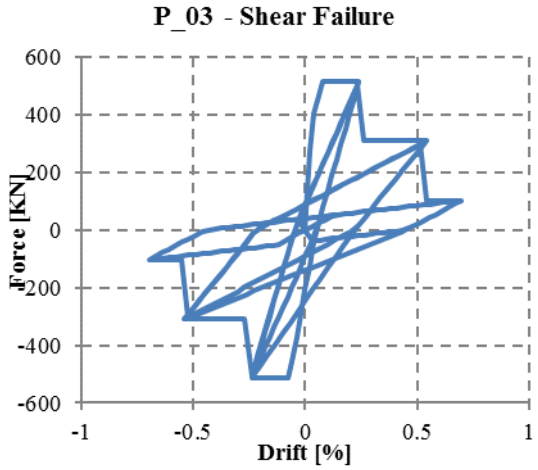

Geometry of the panels	b [m]	h [m]	t [m]	Bound. Cond.
P_01	2.5	2.6	0.3	Double fixed
P_02	3	2.6	0.3	Double fixed
P_03	3.5	2.6	0.3	Double fixed

Figure 7: Example of the cyclic response simulated with the piecewise linear constitutive laws

The nonlinear description of the coupled relation between the flexural and axial degrees of freedom allows the explicit evaluation of how cracking affects the rocking motion. The macroelement model includes a nonlinear degrading model for rocking damage. which accounts for the effect of limited compressive (i.e. toe-crushing) strength.

In addition to geometrical characteristics. the macroelement model is defined by eight parameters representative of an average behavior of the masonry panel: density ρ. elastic modulus in compression E, shear modulus G, compressive strength f_m, shear strength (i.e. cohesion) c_{eff}, global equivalent friction coefficient μ_{eff}, and two coefficients β and c_t. The parameter β governs the slope of the softening branch of the nonlinear shear model, whereas the parameter c_t is a non-dimensional shear deformability. Depending on the macroscopic cohesive behavior, the amplitude of the inelastic displacement component in the displacement–shear relationship is proportional to the product Gc_t (Figure 8).

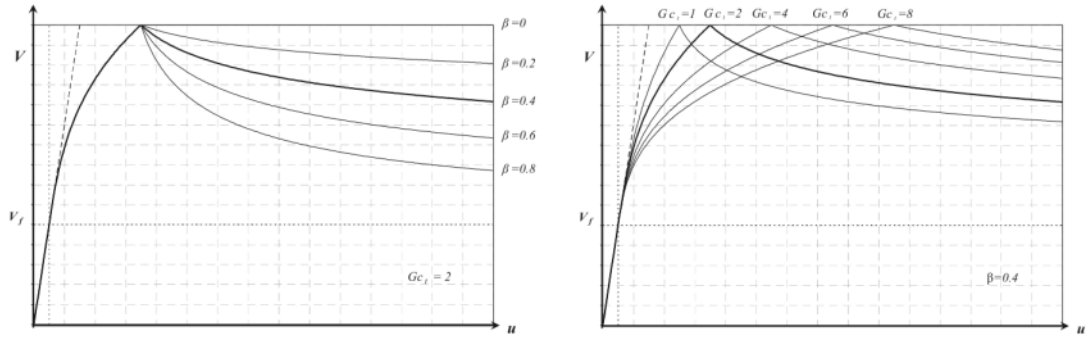

Figure 8: Role of parameters β (left) and c_t (right) on the shape of the nonlinear shear model (Penna et al., 2014).

The macroscopic shear model is based on a combination of equivalent cohesion, c_{eff}, and friction, μ_{eff} parameters. The determination of the model parameters from the "local" mechanical parameters derives from characterization tests and depends on the governing shear failure mode. The parameters of the masonry type used in the numerical models for dynamic analyses were calibrated to be representative of typical unreinforced masonry with perforated clay blocks. The parameters were compared with some literature experimental data (Figure 9, [6]).

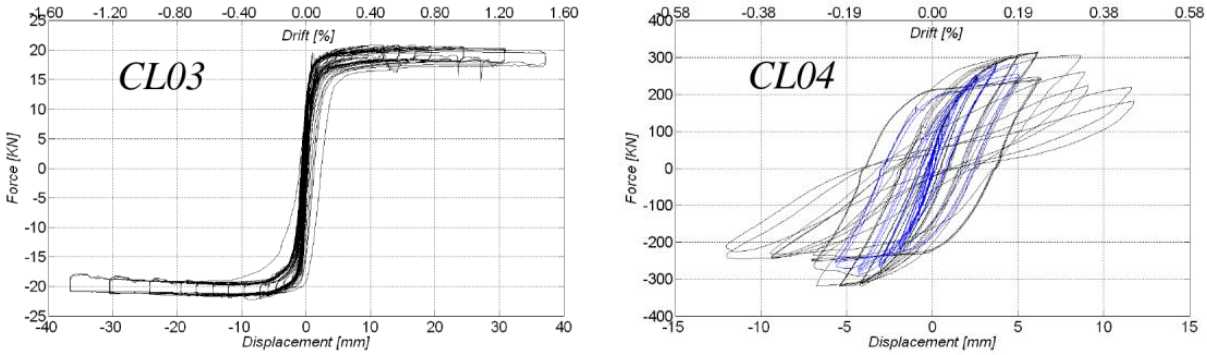

Figure 9: Flexural (left) and shear (right) response of clay-block masonry piers subject to in-plane cyclic shear-compression tests (after [6])

For the analysis of entire buildings, with boundary conditions intermediate between cantilever and double-fixed, an equivalent Young modulus equal to $E' = 2E = 9320$ MPa was used to correctly reproduce the lateral stiffness.

Regarding the shear strength model parameters, the criterion reported in Eurocode 6 was considered. i.e.:

$$V_{res} = l' t f_v \tag{2}$$

with $f_v = f_{vmo} + \mu \frac{N}{l' t} \leq 0.065 f_b$.

The parameters of the macroelement shear model, c_{eff} e μ_{eff}, were calibrated by a linearization of the strength criterion in the proximity of the applied compression level, leading to values of c_{eff} = 0.375 MPa and μ_{eff} = 0.125. The other parameters of the shear model (nonlinear deformation before the peak Gc_t and slope of the softening branch β) were calibrated to derive a cyclic behavior as close as possible to that observed during experimental tests on modern clay block masonry, obtaining $Gc_t = 5$ and $\beta = 0.6$.

The combined effect of flexural and shear failure modes in the building piers generally provide realistic global hysteretic curves for the building models subjected to time history analyses (Figure 10).

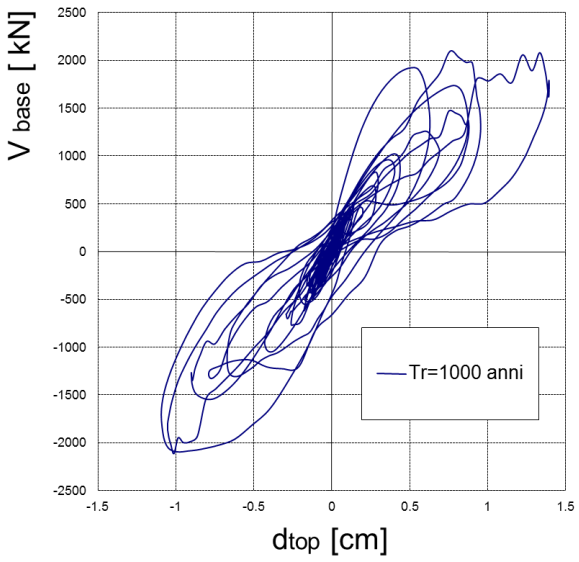

Figure 10: Example of hysteretic base shear-top displacement curve for building E5 (3 stories)

4 ASSESSMENT AND RESULTS

4.1 Definition of the collapse condition

The Engineering Demand Parameter (EDP) selected to identify the performance of the structures is the maximum wall inter-story drift (θ_{max}), computed accounting for the effect of average rotations of the nodes at each storey. Considering the different behavior of the buildings in the two directions, the maximum inter-story drift has been evaluated separately for each of them ($\theta_{max.X}$ and $\theta_{max.Y}$).

Reference thresholds of θ_{max} were defined, for each building configuration and for each direction *X* and *Y*, based on the results of NLSA and NLDA ($\theta_{C,X}$ and $\theta_{C,Y}$). For each direction, the minimum value of θ_{max} corresponding to a 50% global base shear degradation was identified from NLSA carried out with two load patterns (first mode and mass proportional) and in the positive and negative directions. The deformed shape obtained from NLSA was compared with that from NLDA, to check for the possible presence of torsional effects and, in general, their consistency. When the capacity obtained from NLDA highlighted a significant reduction of the maximum inter-story drift, with respect to that obtained from NLSA, the value of θ_{max} was defined by assuming a global base shear degradation of 35% instead of 50%.

The obtained reference thresholds could vary significantly from building to building, due to the activation of different failure modes for different configurations and/or number of storeys. The collapse limit state function was then evaluated, for each building, as:

$$Y_C = max\left\{\frac{\theta_{max.X}}{\theta_{C.X}}; \frac{\theta_{max.Y}}{\theta_{C.Y}}\right\} \tag{3}$$

In case of dynamic instability, associated with lack of convergence of the solution, the huge values of displacement demand provided by the code were checked and this case was eventually indicated as “certain collapse” if a global shear degradation of 90% of the maximum one was observed.

4.2 Results of nonlinear dynamic time history analyses

This section presents some examples of the results obtained from NLDA for the different configurations considered.

Figure 11 shows two examples of the hysteretic response (global base shear vs. average top displacement curves) obtained by NLDA for the site of Naples, soil type C, for the records corresponding to a return period of 1000 and 10000 years, compared with the corresponding pushover curves (both first mode and mass proportional load patterns). For simplicity, only two hysteretic cycles are shown: one is the cycle associated to the time history of the fixed stripe that has produced the maximum top displacement (red curves in Figure 11), while the other is the cycle associated to the time history that has produced the minimum top displacement (blue curves in Figure 11). The significant role of record-to-record variability is evident in the very different structural response produced by records associated to the same return period.

Damage associated to the collapse condition is more concentrated in masonry piers than in spandrels, consistently, as mentioned in §2.1, with the construction details imposed by NTC08 for new masonry buildings. In particular, the presence of rigid diaphragms and r.c. ring beams coupled to spandrels promotes the activation of a Strong Spandrels-Weak Piers (SSWP) behavior. Furthermore, it can be observed that, in most cases, the collapse is reached due to the activation of a soft-story mechanism, generally occurring at the ground level.

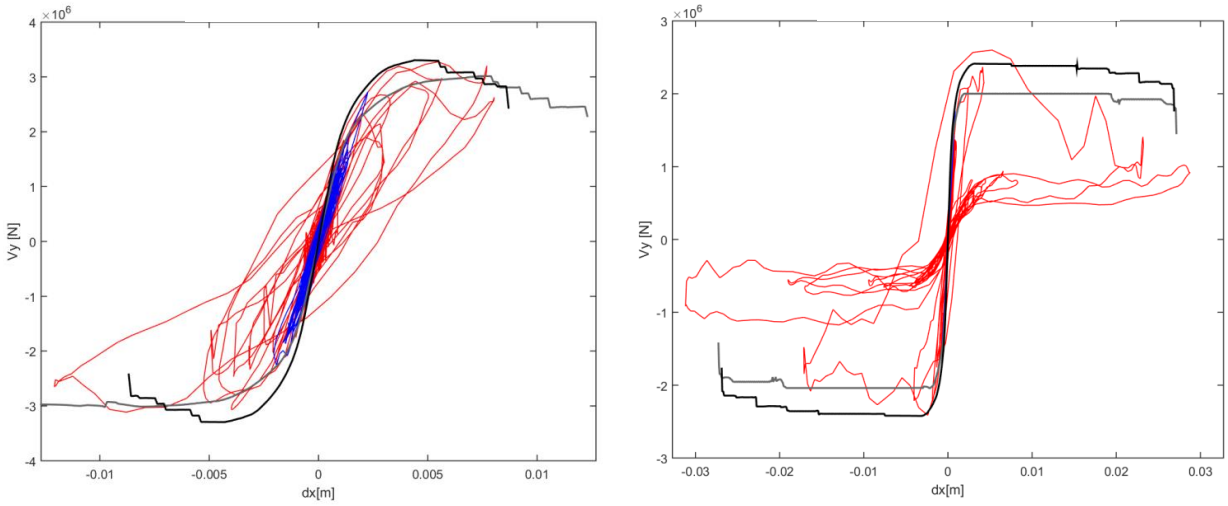

Building C3, 3 stories, Tr = 1000 yrs Building C4, 2 stories, Tr = 10000 yrs

Figure 11: Hysteretic cycles and corresponding pushover curves for the site of Naples, soil type C, X direction.

Figure 12 reports two examples of the results of NLDA in terms of IM-limit state function (Y_C). It is worth noting that the values of Y_C associated with the occurrence of "certain collapse" have been excluded from the graphs. Thus, a lognormal distribution has been assumed for the Y_C values associated with each stripe, to evaluate the 16th, 50th and 84th percentiles. The red curves in the figure were obtained by linearly connecting the corresponding results of the different stripes. The vertical line ($Y_C = 1$) corresponds to collapse.

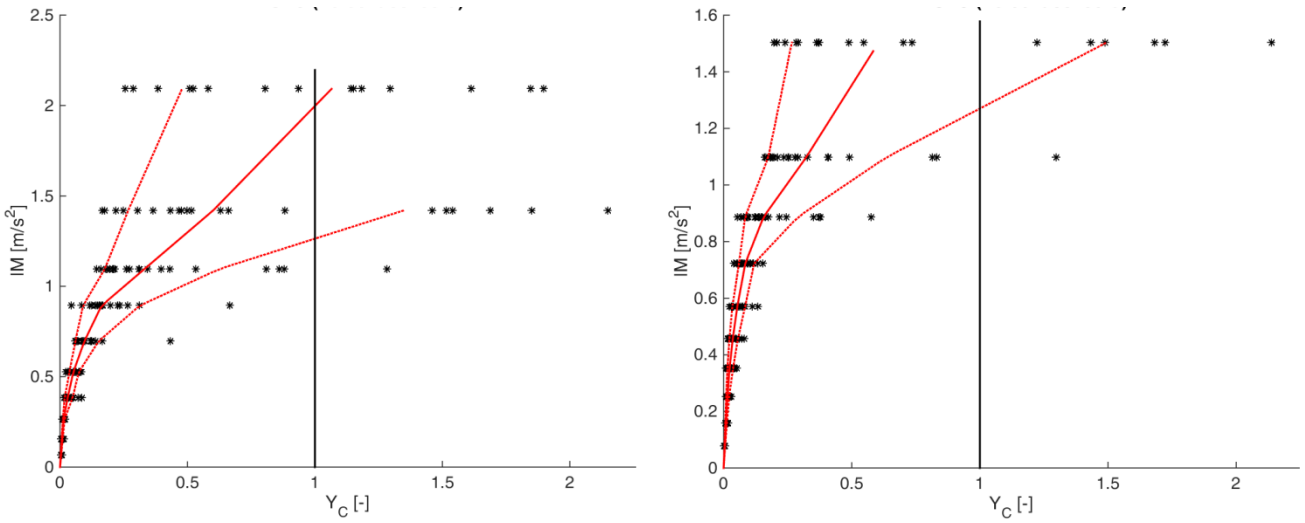

Building C3, 3 stories, Naples, soil type C

Building C4, 3 stories, Rome, soil type C

Figure 12: Results obtained from NLDA in terms of collapse function. Red lines correspond to 16th, 50th and 84th percentiles of the results. The vertical line identifies collapse (Y_C = 1).

Figure 13 compares the percentage of collapses as a function of the return period of the seismic action, obtained for building E8, designed according to different analysis methods, at different sites. It can be qualitatively observed that buildings designed with a linear method show very low failure rates. In many of the cases, no collapses were observed for any of the considered return periods.

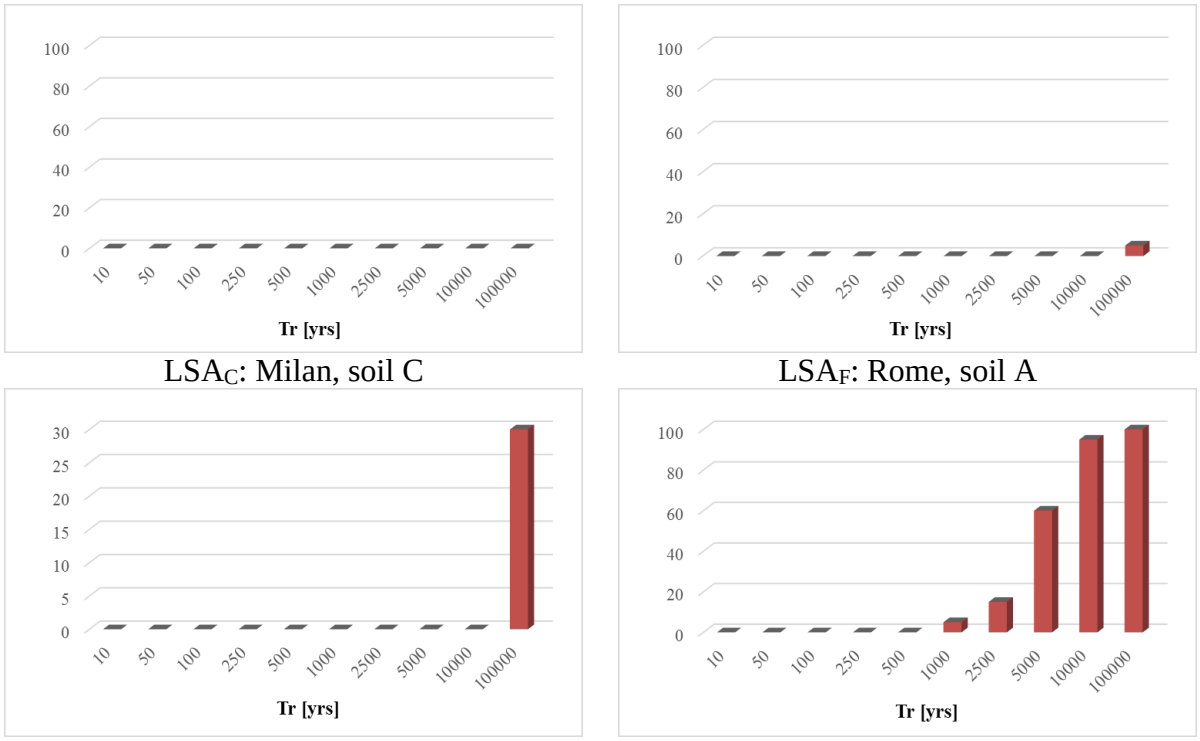

LSA_C: Milan, soil C

LSA_F: Rome, soil A

SB: Naples, soil A

NLSA: L'Aquila, soil C

Figure 13: Percentage of collapses as a function of the return period of the seismic action, obtained for building E8, designed with different analysis methods, at different sites.

These analyses also allowed a quantification of the safety margin provided by the different design methods. Methods based on linear static analysis turned out to be very conservative, whereas those based on "simple buildings" rules were less conservative and those based on nonlinear static analysis were even less conservative. For this last case, the first collapses were observed for 1000 years in most cases (Figure 13).

5 CONCLUSIONS

The design of URM buildings conforming to the recommendation of the Italian Code herein presented highlighted the different safety levels implicitly provided by the different analysis methods (linear static analysis with either equivalent frame or cantilever modeling, nonlinear static analysis with equivalent frame modeling and simple buildings rules).

As apparent from the results presented in [1], the use of linear static analysis resulted to be impractical in many sites, because of an excessive conservatism, in particular if force redistribution is neglected. The adoption of force redistribution could introduce some additional margin, but it is worth pointing out that its application is not straightforward at the engineering practice-level.

On the other hand, in few cases, nonlinear static analyses appeared to be unconservative, especially for building configurations with strong irregularities. This could be due to two main reasons. The first deals with the design parameters (in particular the drift limits associated with shear failure) recommended in NTC08, which are too large for the considered modern masonry typologies (as highlighted by the evidences provided by the increasing number of experimental tests available in the literature) and whose reduction is already foreseen in the draft of revision of NTC. The second deals with the tendency of the N2 method – which is embedded in the nonlinear static assessment procedure - to underestimate the displacement demand for masonry buildings, in case of high values of required ductility [12]. The ongoing research is already addressed to widen all these issues.

ACKNOWLEDGEMENTS

The authors would like to acknowledge the financial support of the Italian Civil Protection Department, through the ReLUIS project 2014-2018 and the EUCENTRE Project 2014-2016.

REFERENCES

[1] I. Iervolino, A. Spillatura, P. Bazzurro, RINTC Project – Assessing the (implicit) seismic risk of code-conforming structures in Italy. COMPDYN 2017 – 6th ECCOMAS Thematic Conference on Computational Methods in Structural Dynamics and Earthquake Engineering, M. Papadrakakis, M. Fragiadakis (eds.), Rhodes Island, Greece, 15-17 June 2017.

[2] NTC08 Decreto ministeriale 14 gennaio 2008: "Norme tecniche per le costruzioni," Ministero delle Infrastrutture, S.O. n.30 alla G.U. del 4.2.2008, No. 29, 2008 – in Italian.

[3] S. Cattari, S. Lagomarsino, Masonry structures. *In: Developments in the field of displacement based seismic assessment*, T. Sullivan and G.M. Calvi (eds.), pp.151-200, IUSS Press Pavia, 2013.

[4] A. Penna, S. Lagomarsino, A. Galasco, A nonlinear macroelement model for the seismic analysis of masonry buildings, *Earthquake Engineering & Structural Dynamics*, **43**(2), 159-179, 2014.

[5] S. Lagomarsino, A. Penna, A. Galasco, S. Cattari, TREMURI program: an equivalent frame model for the nonlinear seismic analysis of masonry buildings, *Engineering Structures*, **56**, 1787-1799, 2013.

[6] G. Magenes, P. Morandi, A. Penna, Experimental in-plane cyclic response of masonry walls with clay units, *Proc. 14th WCEE*, Beijing, China, Paper No. 95, 2008.

[7] P. Morandi, L. Albanesi, G. Magenes G, Prestazioni sismiche di pannelli murari in blocchi di laterizio a setti sottili soggetti a test ciclici nel piano. *Proc. XVI Italian National Conf. on Earthquake Engineering (ANIDIS)*, L'Aquila, Italy – in Italian, 2015.

[8] P. Morandi, L. Albanesi, G. Magenes, In-plane test campaign on different load-bearing URM typologies with thin shell and web clay units, *Proc. 16th International Brick and Block Masonry Conference*, Padua, Italy, 2016.

[9] S. Petry, K. Beyer, Influence of boundary conditions and size effect on the drift capacity of URM walls, *Engineering Structures*, **65**, 76-88, 2014.

[10] W. Mann, H. Müller, Failure of shear-stressed masonry: an enlarged theory, tests and application to shear walls. *Proc. British Ceramical Society*, **30**, 223-235, 1982.

[11] V. Turnsek, P. Sheppard, The shear and flexural resistance of masonry walls. *Proc. International Research Conference on Earthquake Engineering*, Skopje, Macedonia, 1980.

[12] G. Guerrini, F. Graziotti, A. Penna, G. Magenes, Improved evaluation of inelastic displacement demands for short-period masonry structures. *Earthquake Engineering and Structural Dynamics*, DOI: 10.1002/eqe.2862